P3.17   EVALUATION OF CIRRUS PROPERTIES SIMULATED BY A SINGLE-COLUMN MODEL

USING CLOUD RADAR OBSERVATIONS AND RESULTS FROM A CLOUD-RESOLVING MODEL SIMULATION

Yali Luo[*], Steven K. Krueger
Department of Meteorology, University of Utah, Salt Lake City, Utah

Shrinivas Moorthi
Environmental Modeling Center, NCEP, NOAA, Camp Springs, Maryland

1. INTRODUCTION

Using cloud radar observations of cirrus cloud properties obtained at the ARM (Atmospheric Radiation Measurement program) SGP (Southern Great Plains) site and results from a CRM (cloud-resolving model) simulation, we are evaluating the cirrus properties simulated by a SCM (single-column model). The SCM is based on the NCEP (National Centers for Environmental Prediction) MRF (Medium Range Forecast) model, which includes cloud water/ice as a prognostic variable. We used SCM and CRM simulations based on intensive observations made at the ARM SGP site for 29 days from 19 June to 17 July 1997. During this period, cirrus clouds, many generated by deep convection, were observed about 30 percent of the time by the cloud radar.

To produce cirrus statistics from the SCM results that are comparable to the cloud radar observations, we used a method described by Klein and Jakob (1999) that uses the SCM cloud fraction profile and the SCM's overlap assumption (random or maximum/random) to create a synthetic cloud field. The SCM's cloud water/ice is assumed to be uniformly distributed in the clouds at each level. We then sampled the synthetic cloud fields like a cloud radar would to determine the statistical properties of "cirrus" and "thin cirrus", as defined by Mace et al. (2001). We compared the SCM's cirrus cloud properties to those obtained by Mace et al. using the ARM cloud radar and the corresponding CRM simulation.

2. SCM SIMULATION

2.1 *NCEP MRF SINGLE-COLUMN MODEL*

The single-column model (SCM) used is based on the National Centers for Environmental Prediction (NCEP) Medium Range Forecast (MRF) model. Recent

* Corresponding author address: Univ. of Utah, Dept. of Meteorology, Salt Lake City, Utah 84112. Email: yali@met.utah.edu

description about the NCEP MRF model can be found from Kalnay et al. (1998).

The stratiform cloud condensate mixing ratio, which can be either liquid water or ice depending on local temperature and cloud top temperature, is predicted explicitly in the SCM. In the model, the processes effecting the cloud condensate include three dimensional advection, grid-scale condensation (Zhao and Carr 1997), convective detrainment at cloud top (Pan and Wu 1995), conversion of cloud condensate to precipitation (Zhao and Carr 1997 for ice, and Sundqvist et al. 1989 for liquid water), evaporation of cloud condensate (Zhao and Carr 1997), and horizontal and vertical diffusion.

For radiation calculation, the fractional area of the grid point covered by the cloud, i.e. cloud fraction, is diagnosed from the predicted cloud condensate mixing ratio and relative humidity following Xu and Randall (1996). The effect of convection on cloud fraction is included through the detrainment of cloud condensate by convective mass flux. The fractional cloud cover is allowed at all model levels and clouds are assumed to be randomly overlapped for radiation calculation.

In the SCM, the shortwave radiation includes absorption/scattering by water vapor, ozone, carbon dioxide, and clouds based on the work of Slingo (1989), Chou et al. (1998) and Kiehl (1998). The infrared radiation follows Kiehl et al. (1998) and Stephens (1984). The cloud radiation heating rate is calculated using the predicted cloud condensate. Clouds on different model levels are randomly overlapped.

Penetrative convection in the SCM is simulated following Pan and Wu (1995), which is based on Arakawa-Schubert (1974) as simplified by Grell (1993) and with a saturated downdraft. The key variable is cloud work function, which is determined by the temperature and moisture in each air column of the model gridpoint. Convection occurs when the cloud work function exceeds a threshold. Mass flux of the cloud is determined using a quasi-equilibrium assumption based on this threshold cloud work function. The temperature and moisture profiles are adjusted towards the equilibrium cloud work function within a specified time scale using the deduced mass flux. This scheme allows the transportation of momentum, as well as heat and moisture, by the mass fluxes induced in the updraft and the downdraft. Only the deepest cloud is considered as a

major simplification to the original Arakawa-Schubert scheme in which a spectrum of clouds are considered. A level between the highest possible cloud top, which is determined by the parcel method, and the level where environmental moist static energy is minimum is selected randomly as the cloud top.

2.2 *SCM SIMULATION DESCRIPTION*

The MRF SCM was run for 29 days (from June 18 23:30 UTC to July 17 23:30 UTC 1997). The large-scale data set of the ARM summer 1997 SCM IOP at the SGP cloud and radiation testbed (CART) site produced by the variational analysis method (Zhang et al. 2001) was used to drive the model.

The model was set to have 28 unequally-spaced sigma levels with about 20 levels in the troposphere. The predicted variables were updated every half an hour and radiation parameterization was calculated every timestep. The advection of cloud condensate was not included due to lack of observation.

The SCM predicts too warm atmosphere at all levels. The mean errors of temperature are large at upper and low troposphere (4 K and 2 K respectively) and small in the middle layer, i.e. 600 to 400 mb. The root-mean-square (RMS) error of temperature is about 5 K, comparable to the CRM's results (Xu and Randall 2000). It predicts too moist atmosphere in middle to upper levels. The RMS error of relative humidity is about 30% and the bias about 25%. To compare, the CRM over-predicted relative humidity at middle to upper levels, too, but with lower RMS error (20%) and bias (10%).

3. OBSERVATIONS

The macrophysical properties of cirrus observed by the MMCR and microphysical properties of "thin cirrus" retrieved by Mace et al (2001; MCA hereafter) for the summer 1997 (June, July, and August) were used in our analysis. We describe the retrievals shortly here. Similar descriptions can be found in Mace et al. (2001) and Luo et al. (2002).

According to MCA, to qualify as a cirrus cloud layer, the temperature at cloud top must be less than -35°C and the temperature at the level of maximum ice water content (IWC) must be less than -20°C. This definition ensures that ice microphysical processes are dominant in the generation region near cloud top, but excludes deep cloud layers that are capped by ice-phase clouds. MCA used a version of this definition based on radar reflectivity. They required the radar echo top to occur at a temperature less than -35°C and the level of maximum dBZ_e to occur at a temperature less than -20°C. At cirrus cloud levels, the minimum detectable reflectivity of the SGP cloud radar is -40 to -35 dBZ_e. The temporal and vertical resolution of the cloud radar is 30 s and 90 m, respectively.

MCA retrieved the ice water path (IWP), layer mean effective radius (r_e), and the layer mean ice particle concentration (n) using the method described by Mace et al. (1998). The method assumes that the cirrus ice particle size distribution can be described by a first-order modified Gamma distribution. The particular size distribution is determined by requiring that its sixth moment match the observed radar reflectivity factor, and that its radiative properties, as parameterized by Fu and Liou (1993), match the radiance measured by the atmospheric emitted radiance interferometer (AERI) at wavelength between 10.2 to 12.5 microns. This retrieval algorithm requires that the cirrus layer be optically thin, with a layer emittance less than 0.85. It is also necessary that no lower clouds obscure the cirrus layer from the AERI. The temporal resolution of the retrieved properties is determined by the AERI: 3-minute averages are generated every 8 minutes, so these numbers represent the individual retrievals which are 3 minute averaged layer means.

4. CRM SIMULATION

The cloud resolving model used in this study is the 2-D UCLA/CSU (University of California at Los Angeles/ Colorado State University) CRM. The details of the CRM have been described by Krueger (1988), Xu and Krueger (1991), and Xu and Randall (1995). The dynamics of the CRM is based on the anelastic system. The physical parameterizations in the model consist of a third-moment turbulence closure, a bulk three-phase microphysics, and an interactive solar and IR radiative transfer scheme.

The description of the bulk microphysics of the CRM can be found in Fu et al. (1995), Krueger et al. (1995), Lord et al. (1984), Lin et al. (1983), and Hsie et al. (1980). The bulk microphysics includes five species: cloud water, cloud ice, snow, graupel, and rain. In the CRM, cirrus clouds contain small ice crystals ("cloud ice") and large ice crystals ("snow").

The same data set used to driven the SCM were used to drive the CRM (Xu and Randall 2000). The simulated cirrus properties were compared with MCA's results (Luo et al. 2002). The excellent qualitative agreement between the CRM simulation and the observed cirrus statistics is evident. These are proofs that the essential physics of cirrus formation, maintenance, and decay are exhibited in the CRM simulation.

5. ANALYSIS OF SCM RESULTS

The SCM predicts cloud condensate (liquid water or ice) which represents a grid mean value, i.e. on the scale of hundred kilometers. The cirrus properties from cloud radar observations and the retrievals represent values on kilometer scale. The SCM results can not be compared directly to the cloud radar observations and retrievals because of this scale discrepancy. We need to distribute the SCM results into subcolumns for such

comparison. In our study, two extreme situations are analyzed. As one extreme situation, the effects of snow and rain are neglected completely, i.e. the SCM cirrus clouds consist of cloud ice only and, only cloud ice or cloud liquid water is considered to calculate the reflectivity. This situation is called NOSNOW situation. In the other situation, the SCM cirrus clouds consist of both cloud ice and snow. In addition to cloud ice and cloud water, snow and rain are included for reflectivity calculation. Snow and rain are assumed to distribute uniformly in snowy and rainy areas, which are determined based on the microphysics in the SCM. This is called SNOW situation.

5.1 *NOSNOW ANALYSIS*

The SCM predicted cloud condensate at all model levels was subdivided into 100 subcolumns using an overlap assumption basically following the method described by Klein and Jakob (1999). Thus a cloud configuration was generated each time. Different overlap assumptions generate different cloud configurations. Maximum/random and random overlap assumptions are two assumptions most commonly used in current large-scale models. The random overlap assumptions is used in the SCM, which means the positions of cloudy cells at each level is determined randomly. The maximal/random overlap means that when clouds occur in adjacent layers, they are maximally overlapped but the excess portion is positioned at random across the layer. In addition, if a clear layer separates two cloudy layers, they are assumed to be randomly overlapped. In our analysis both maximum/random and random overlap assumptions were used for NOSNOW analysis. Figure 1 gives an example of the cloud configurations generated by using these two assumptions. This method was applied to the SCM simulated profiles of cloud condensate and cloud fraction every hour over the entire simulation period. Neglecting horizontal inhomogeneity, the "local" cloud condensate mixing ratio is $\frac{\bar{q}_c}{C}$, where $\bar{q}_c$ is the grid mean cloud condensate mixing ratio and C is cloud fraction.

For each subcolumn, the reflectivity is calculated from cloud ice or cloud liquid water content using the following equation suggested by S. Matrosov (personal communication):

$$Z_e = aWr_e^3 \qquad (1)$$

where Z_e is reflectivity factor in mm^6 m^{-3}, a is a coefficient (49.6x10^{-6} for liquid, 9.4x10^{-6} for ice), W is

liquid or ice water content in g m^{-3}, and r_e is an effective radius of the cloud particles in micrometers (Beesley et al. 2000). In the SCM, r_e depends on temperature. For cloud ice, r_e equals 20 μm at temperatures lower than 223.26 K, and increases to 80 μm at 263.26 K. For cloud water, r_e is 5 μm at temperatures warmer than 273.16 K, and increases to 10 μm at 253.16 K. The same method to determine r_e is used in our analysis.
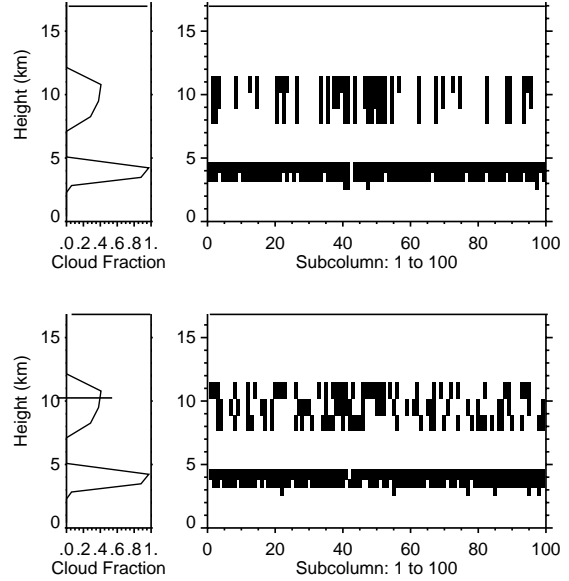
Figure 1. An example of cloud distribution obtained by combining the SCM simulated cloud fraction with an overlap assumption. Top panel: maximal/random overlap assumption; bottom panel: random overlap assumption.

The IR emissivity of a cirrus layer is computed for each subcolumn from the mixing ratios and effective sizes of cloud ice. The cloud layer IR emittance ε at a particular wavelength is defined as

$$\varepsilon = 1 - \exp\left[-\int_{z_1}^{z_2} \sigma_a(z)dz\right], \qquad (2)$$

where

$$\sigma_a(z) = [1 - \tilde{\omega}(z)]\beta(z), \qquad (3)$$

is the infrared absorption coefficient, z_1 is the cloud base height, z_2 is the cloud top height, $\tilde{\omega}$ is the single-scattering albedo, and β is the extinction coefficient. As parameterized by Fu and Liou (1993), β and $\tilde{\omega}$ can be obtained in terms of the mean effective size and ice water content:

$$\beta = IWC \sum_{n=0}^{2} a_n / D_e^n \qquad (4)$$

$$1 - \tilde{\omega} = \sum_{n=0}^{3} b_n D_e^n, \qquad (5)$$

where a_n and b_n are wavelength-dependent coefficients, and D_e is the mean effective size of ice crystals. Fu and Liou gave the coefficients for 18 spectral bands with central wavelengths ranging from 0.55 to 70.0 micrometers. In order to match the radiance used by MCA (wavelength between 10.2 to 12.5 microns), those coefficients for the spectral band with 11.3 microns central wavelength are used in our calculation.

We then sampled cirrus and "thin cirrus" at the 100 subcolumns, neglecting the effects of snow and rain, using nearly the same definition of cirrus and "thin cirrus" as MCA, and analyze their properties.

5.2 *SNOW ANALYSIS*

The cloud radar saw all hydrometers, so that snow should be included as part of cirrus and the effects of snow and rain on reflectivity should be considered. However, the SCM does not predict snow mixing ratio and rain mixing ratio. It predicts snow flux and rain flux at each level, instead. Based on the microphysics in the SCM, we diagnosed mixing ratios of snow and rain from their fluxes.

In the SCM, it is assumed that net snow generation in one level is assumed to be balanced by snow net falling out in one time-step, i.e. the equation

$$S_{micro} = \frac{1}{\rho}\frac{\partial}{\partial z}(\rho \overline{V_s q_s}) \qquad (6)$$

holds, where S_{micro} is the net snow generation by microphysical processes, V_s is snow falling speed, and q_s is the "local" snow mixing ratio, $\rho \overline{V_s q_s}$ is the grid mean snow flux ($\overline{P}_s$). By assuming that snow distributes uniformly in snowy area, we get

$$P_s \equiv \rho \overline{V_s(q_s)q_s} = \rho V_s\left(\frac{\overline{q_s}}{\sigma_s}\right)\overline{q_s}, \qquad (7)$$

where $\overline{q}_s$ is the grid mean snow mixing ratio, σ_s is the snow fraction, i.e. the area covered by snow in the SCM grid. The snow falling speed is a function of its local mixing ratio. The formula for snow falling speed used by the University of Utah Cloud Resolving Model (UU CRM) is used here and its derivation can be found in Lin et al. (1983) and Luo et al. (2002):

$$V_s\left(\frac{\overline{q_s}}{\sigma_s}\right) = 1.8355198\left(\rho\frac{\overline{q_s}}{\sigma_s}\right)^{0.0625}\left(\frac{\rho_{sfc}}{\rho}\right)^{0.5}. \qquad (8)$$

Combining equations (7) and (8), we get

$$\overline{q}_s = \left[\frac{\overline{P}_s\sigma_s^{0.0625}}{1.8355198\rho_{sfc}^{0.5}\rho^{0.5625}}\right]^{1/1.0625}. \qquad (9)$$

Equation (9) means the grid mean snow mixing ratio can be diagnosed from grid mean snow flux and snow fraction, so that the snow fraction σ_s needs to be determined first. In the SCM, source terms for snow include a) snow falling from above, b) autoconversion of cloud ice to snow, and c) accretion of cloud ice by snow. Based on this, we can determine a sub-grid cell is snowy or not based the cloud distribution at that level and the distribution of snow above as indicated by figure 2:
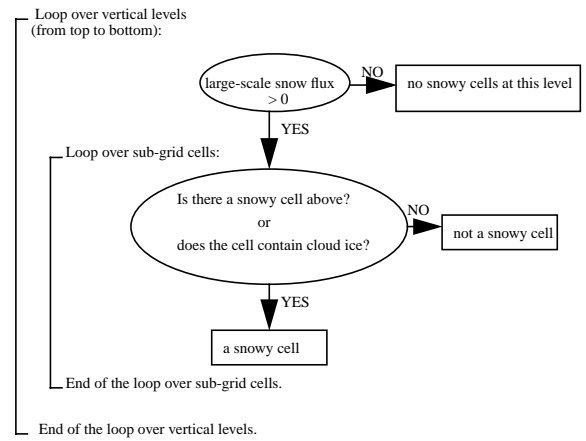
Figure 2. The flow chart of the method to determine whether a subgrid cell is snowy or not.

Thus a snow distribution can be determined and at the same time we get the snow fraction which is the number of snowy cells divided by the total number of cells.

In the SCM, rain at a level comes from rain falling from above, conversion from cloud liquid water, and snow melting. We determine each cell is rainy or not using similar method as figure 2. We then get rain mixing ratio by relating it to rain falling speed and neglecting the horizontal inhomogeneity of rain distribution. Again the falling speed for rain used in the UU CRM is used in our calculation.

The reflectivity of snow is computed as cloud ice with r_e equals 75 μm. For rain, the following equation is used:

$$Z_e = 3071.29 W^{1.75} 0.08^{-0.75}, \qquad (10)$$

where W is rain content in g m^{-3}.

We sampled cirrus and "thin cirrus" at the 100 subcolumns each hour, including the effects of snow and rain, using nearly the same definition of cirrus and "thin cirrus" as MCA, and analyze their properties.

6. RESULTS

When neglecting snow and rain (NOSNOW analysis), 25,620 cirrus samples and 13,058 "thin cirrus" samples were found. The numbers decrease to 11,930 and 7,417 for SNOW analysis. The cloud occurrence frequency (COF), location, thickness, and mid-cloud temperature, for both cirrus and "thin cirrus" clouds were analyzed statistically and compared to the MMCR observations and the CRM simulation. In addition, for "thin cirrus" clouds, the ice water content (IWC), ice water path (IWP), effective radius (r_e), IR emittance, and visible optical depth were also evaluated statistically.

6.1 *CIRRUS CLOUD OCCURRENCE FREQENCY*

The SCM cirrus and "thin cirrus" cloud occurrence frequency (COF) was calculated as the fraction of subcolumns where cirrus and "thin cirrus", respectively, occurred in the model. For the cloud radar observations, the cirrus and "thin cirrus" COF was the fraction of time when cirrus cloud and "thin cirrus" cloud was observed, respectively. For one column of CRM, the cirrus COF was calculated the same as for the radar observations. The cirrus COFs at 16 evenly-distanced columns in the CRM was averaged to get the domain-mean (i.e. large-scale) value. The GOES high cloud amount during the IOP is also used for comparison.

Over the entire simulation period SCM NOSNOW cirrus clouds had a mean COF of 25% and 37% when maximum/random and random overlap assumptions

were used, respectively, SNOW cirrus clouds (random overlap only) occur 17% of time. Compared to the observations (cloud radar 30% and GOES 27%), the SCM SNOW analysis and NOSNOW with maximum/random overlap assumption analysis underestimated the occurrence of cirrus, while NOSNOW with random overlap assumption analysis overestimated it.

Table 1. Values without brackets or parentheses are cirrus occurrence frequency from the MRF SCM simulation, the CRM simulation, radar observations (Mace et al. 2001), and GOES observation at ARM SGP CART site. Values in brackets are correlation coefficients and values in parentheses are normalized standard deviation, with respect to GOES high cloud amount.

Period	Entire IOP	Subperiods A, B, C
SCM max/rand (cloud ice)	0.25 [0.44] (1.02)	0.25 [0.54] (1.01)
SCM rand (cloud ice)	0.37 [0.47] (1.29)	0.33 [0.68] (1.20)
SCM rand (cloud ice & snow)	0.17 [0.09] (0.94)	0.17 [0.22] (0.89)
CRM	0.37 [0.30] (1.25)	0.30 [0.70] (1.01)
MMCR	0.30 [0.63] (1.52)	0.37 [0.63] (1.48)
GOES	0.27 [1.00] (1.00)	0.34 [1.00] (1.00)

The 3-hourly COFs for the SCM, radar observations, and the CRM domain-mean values were calculated and compared to the GOES observed 3-hourly high cloud amount (Minnis et al. 1995) during the simulation period. Table 1 gives their mean COFs, the correlation coefficients and normalized standard deviations with respect to the GOES high cloud amount. Both the entire simulation period and selected subperiods, during which clouds were formed mainly locally and which covers about half of the entire simulation period, are considered. For the entire simulation period, the correlation coefficients for SCM NOSNOW cirrus are 0.44 and 0.47 using maximum/random and random overlap assumption, respectively, the SCM SNOW (random) 0.09, while that for cloud radar observed cirrus is 0.63 and the CRM cirrus 0.30. When only the selected subperiods were considered, the two correlation coefficients for SCM NOSNOW cirrus increased from 0.44 to 0.54 (maximum/random) and 0.47 to 0.68 (random) respectively, SCM SNOW (random) from 0.09 to 0.22, the CRM from 0.30 to 0.70, while the cloud radar observations did not show such a change. Since the SCM and the CRM consist of very

different physics, the increase of COF found in both models indicate the detrimental effects of lack of hydrometer advection into or out of the model's domain on the simulated cirrus occurrence. When random overlap assumption was used, the SCM NOSNOW cirrus COF correlated a little bit better with the GOES high cloud amount (and with radar observed cirrus COF) than with NOSNOW maximum/random cirrus, and much better than SNOW (random) cirrus. The poor correlations between SNOW random cirrus and the observations (0.09 for the entire IOP and 0.22 for the selected subperiods), compared with those between NOSNOW random and observations (0.47 and 0.68), is due to the over-estimation of the SCM snow fraction which excluded many subcolumns as cirrus.

6.2 *CIRRUS MACRO-SCALE STATISTICS*

The frequency distributions of cirrus cloud top heights, cloud base heights, cloud thickness, and mid-cloud temperature are shown by figure 3. In the figure, the solid lines represent radar observations, dotted lines represent CRM results, dash-dotted lines represent the SCM SNOW random results, and thin solid lines are for the SCM NOSNOW random results. (SCM NOSNOW maximum/random results are not shown in figure 3 since they are very similar to NOSNOW random results.) Table 2 gives the statistics of these macro-physical properties.

In the NOSNOW analysis, regardless of the overlap assumption used, the depth of the thinnest SCM cirrus and "thin cirrus" clouds is about 1.1 km determined by the vertical resolution of the SCM at the cirrus levels.
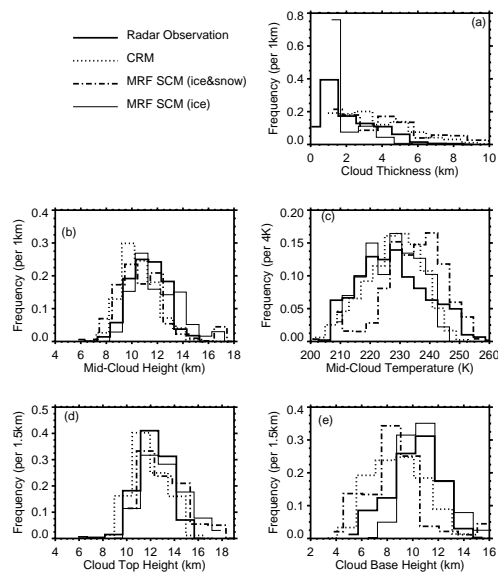
Both the SCM cirrus and "thin cirrus" clouds have modes at the possible thinnest depth. About 75% (random) and 50% (maximum/random) of the NOSNOW cirrus and "thin cirrus" clouds are thinner than 2 km, i.e. they occur at a single model level. The cirrus cloud base heights are too high compared to observations and CRM simulation because snow is not considered.

When random overlap assumption was used, the SCM NOSNOW cirrus and "thin cirrus" clouds had higher cloud base heights and mid-cloud heights, and they were physically thinner and had lower mid-cloud temperature, compared to the SCM NOSNOW cirrus and "thin cirrus" clouds when maximum/random overlap assumption was used (table 2). These results are due to the tendency that maximum/random overlap assumption generates thicker cloud, when there are clouds existing at contiguous levels, than random overlap assumption.

SNOW analysis gives too low cirrus cloud base height and too large cloud thickness due to snow extending too low.

Table 2: Cirrus macro-scale statistics derived from the MRF SCM simulation and CRM simulation over summer 1997 SCM IOP period and from Mace et al. (2001) summer 1997 (June, July, August) data at the SGP ARM site. The values outside of brackets or parentheses are mean quantities, values in parentheses denote standard deviations of the mean quantities and values in brackets denote means derived from the optically thin single layer subset of cloud events. *: The cirrus cloud frequency is obtained using data during the SCM Summer IOP period.

Figure 3. Frequency distributions of "all cirrus" (a) cloud thickness, (b) mid-cloud height, (c) mid-cloud temperature, (d) cloud top height, and (e) cloud base height. Solid line: radar retrievals; dotted line: CRM results; dash-dotted line: SCM SNOW random results; thin solid line: SCM NOSNOW random results.

	SCM max/ rand (cloud ice)	SCM rand (cloud ice)	SCM rand (cloud ice & snow)	CRM	MCA
Freq. (%)	25 [15]	37 [19]	17 [11]	37 [19]	30* [16*]
Base Height (km)	10.3 (1.7) [10.4]	11.1 (1.9) [11.0]	8.7 (2.7) [8.5]	8.8 (2.0) [8.9]	10.3 (1.8) [10.8]
Top Height (km)	13.0 (1.9) [12.9]	12.9 (1.8) [12.8]	12.9 (1.9) [12.9]	12.0 (1.3) [11.7]	12.1 (1.4) [12.4]
Mid-Cloud Height (km)	11.7 (1.6) [11.6]	12.0 (1.8) [11.9]	10.8 (2.0) [10.7]	10.5 (1.3) [10.3]	11.2 (1.5) [11.6]
Thickness (km)	2.7 (1.7) [2.4]	1.8 (0.8) [1.8]	4.2 (2.5) [4.4]	3.4 (2.0) [2.8]	2.0 (1.5) [1.5]
Mid-Cloud Temperature (K)	230 (8.1) [230]	227 (9.2) [228]	235 (10.3) [236]	228 (9.4) [228]	225 (10.5) [223]

6.3 *"THIN CIRRUS" MICRO-SCALE STATISTICS*

6.3.1 *FREQUENCY DISTRIBUTIONS*

The frequency distributions of microphysical properties (IWP, IWC, and r_e) for "thin cirrus" clouds are given by figure 4. For the SCM, only the results with random overlap assumption are shown.
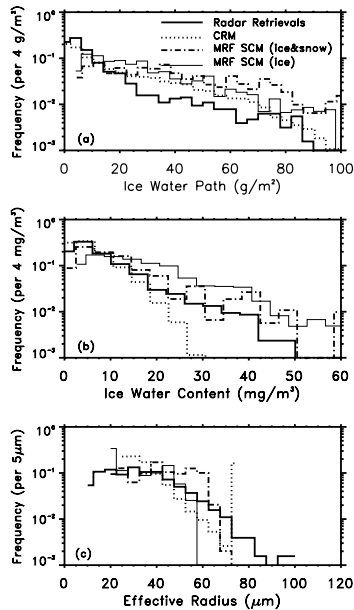
Figure 4. Frequency distributions of "thin cirrus" (a) ice water path, (b) layer-mean ice water content, and (c) layer-mean effective radius. Solid line: radar retrievals; dotted line: CRM results; dash-dotted line: SCM SNOW random results; thin solid line: SCM NOSNOW random results.

Figure 4 shows that for "thin cirrus" clouds, no matter snow is considered or not, the SCM IWP and IWC distributions are too large except at low values of IWP or IWC, respectively, i.e. cirrus with large IWP or IWC occur too often relative to cirrus with low IWP. Their mean, mode, and median values are too large compared to the retrievals and CRM results. The distribution of the layer-mean effective radius (r_e) covers too narrow a range with no values larger than 75 μm. Based on these results, it is not surprising that the SCM "thin cirrus" had too large IR emittance and visible optical depth (not shown).

The distributions of the SCM NOSNOW "thin cirrus" IWC, IWP and r_e did not change much with the overlap assumption used. Random overlap assumption generates results which are a little bit closer to those of the retrievals: relatively a little bit more samples with smaller IWC, IWP, IR emittance, and visible optical depth.

6.3.2 *DEPENDENCE ON TEMPERATURE*

The layer-mean IWC and IWP of the SCM "thin cirrus" clouds were divided into 8 different temperature bins using a 5 K bin size. The mean values of the IWC and IWP in each temperature bin and their 90 percent confidence intervals were calculated and compared to the retrievals and CRM simulation (figure 5). As show by figure 5, the SCM "thin cirrus" clouds contain too large IWC and IWP, except for the coldest temperature bin (207.5 - 212.5 K), i.e. their IWP and IWC increase too rapidly with temperature. The CRM "thin cirrus" IWP is very close to the retrievals, but its IWC is too low due to too large cloud layer thickness. Again, NOSNOW with maximum/random overlap assumption results (not shown) are very close to NOSNOW with random overlap assumption.
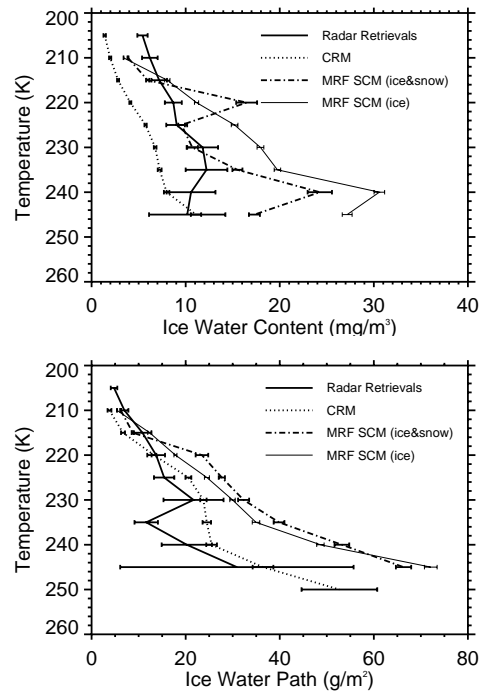
Figure 5. "Thin cirrus" micropysical properties as function of temperature. (a) ice water content, (b) ice water path. Solid line: radar retrievals; dotted line: CRM results; dash-dotted line: SCM SNOW random results; thin solid line: SCM NOS-NOW random results.

6.3.3 *DEPENDENCE ON CLOUD DEPTH*

The layer-mean IWCs and IWP of the retrieved warm ($\bar{T}$ > 230 K), neutral (220 K < $\bar{T}$ < 230 K), and cold ($\bar{T}$ < 220 K) "thin cirrus" clouds were segregated by the cloud physical depth into 3 classes: 0 - 1km, 1 -2 km, 2 - 4 km. Similarly, for the SCM warm, neutral, and cold "thin cirrus" clouds respectively, the layer-mean IWCs were divided into 3 different classes by the cloud

physical depth: thin (1 - 2 km), neutral (2 - 4 km), and thick (4 - 6 km). Note that the vertical resolution of the SCM at "thin cirrus" levels is about 1.1 km so the cloud depth can not be less than 1 km. Figure 6 gives the comparison of IWC between the SCM, the CRM and the observed "thin cirrus".

The red lines in figure 6 represent results from the retrievals. The green lines in figure 6 represent the SCM SNOW results with random overlap assumption, the yellow lines represent SCM NOSNOW results with random overlap assumption, and the blue lines are CRM results. Basically, figure 6 tells us two things. One is that IWCs incerase with temperature as revealed by the SCM, CRM and observation, but the increasing rate is too high in the SCM (as already shown by figure 5). This resulted in too large IWCs for the SCM warm "thin cirrus" clouds. The other thing is that the SCM "thin cirrus" IWCs decrease with cloud thickness, which is opposite to the retrievals and CRM results which show layer-mean IWCs increasing with cloud thickness. The mean IWCs contained in the SCM NOSNOW "thin cirrus" clouds with depths less than 2 km is about 2 times as large as those contained in thick (4 - 8 km) SCM NOSNOW "thin cirrus" clouds, in all of the three temperature classes. The IWCs of the thin SCM "thin cirrus" clouds are even higher when maximum/random overlap assumption was used (not shown).
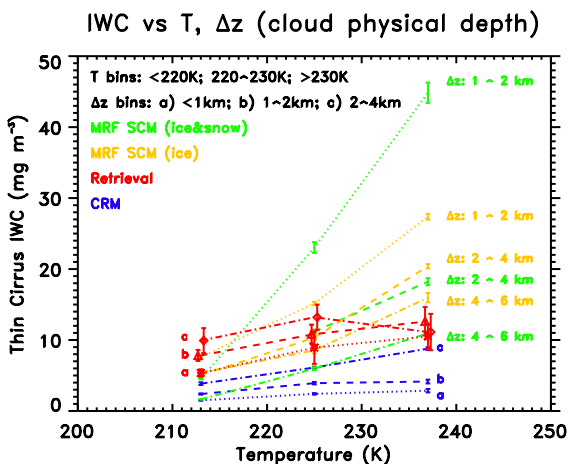
Figure 6. "Thin cirrus" layer-mean ice water content in three temperature bins and three cloud thickness bins. Red: retrievals; blue: CRM results; green: SCM SNOW random results; yellow: SCM NOSNOW random results.

The retrievals, CRM results, and SCM results all show that "thin cirrus" IWPs increase with temperature and cloud depth (not shown). Again, the SCM "thin cirrus" IWPs increase too fast with temperature.

Most of the SCM NOSNOW "thin cirrus" clouds had thickness less than 2 km. When random overlap assumption was used, 10,217 samples, i.e. 78% of the total samples, were found to have thickness less than 2 km. The number decreased to 5,782 (56%) when

maximum/random overlap assumption was used. Properties of these SCM NOSNOW "thin cirrus" clouds influence significantly the statistics of the total samples. These NOSNOW "thin cirrus" clouds occurred at only one model level in the SCM. By tracing the change of IWC in the model, we found that these thin "thin cirrus" clouds were generated originally by detrainment from deep convection. The results here suggest that just-detrained cirrus clouds contain too much ice content.

7. CONCLUSIONS AND DISCUSSION

Compared with the observations, over the entire simulation period, with the random overlap assumption the SCM NOSNOW cirrus COF is too large while with maximum/random overlap assumption it is too small, and the SCM NOSNOW cirrus occurrence was found to correlate temporally all right to the GOES high cloud amount. When subperiods during which clouds were formed mainly locally were considered, the correlation increased to 0.68 (with random overlap assumption) and 0.54 (with maximum/random overlap assumption), which are comparable to that of the radar observations (0.63). The correlation coefficient of the CRM cirrus COF increases, too, from 0.30 to 0.70 while those of the MMCR observations does not show such a increase. Because snow fraction is over-estimated and snow extends too low, SNOW analysis decreases the cirrus mean COF to about half of the SNOW analysis results and results in poor temporal correlation with the observations.

NOSNOW SCM cirrus clouds have too high cloud base hight and many of them occur at a single model level. SNOW cirrus clouds have too low cloud base height and too large cloud thickness.

Regardless of the overlap assumption used: the SCM NOSNOW and SNOW cirrus clouds had too high cloud top heights probably due to too moist model atmosphere at cirrus levels; for the SCM NOSNOW and SNOW "thin cirrus" clouds:

a) large IWP and large layer-mean IWC occur too often relative to small IWP and IWC resulting in too large mean IWP and IWC. One possible reason is that the just-detrained cirrus clouds, which contain too much ice, have too large cloud fraction in the SCM. The time-height distributions (not shown) of SCM cloud ice mixing ratio, detrainment rate of cloud ice, and cloud fraction show maximum values at same time and height. These maximum values occur at one single level over too short time, while the CRM results show much smoother distribution. This supports our hypothesis. To further check this hypothesis, we plan to compare the SCM simulated frequency distributions of cloud fraction and cloud ice mixing ratio at cirrus levels to the CRM results.

b) the IWP and layer-mean IWC are too large at most temperature bins considered except at temperatures lower than 215 K, and they increase with temperature too fast; One possible reason is that the SCM cirrus clouds with large IWP and IWC last too long

and those with small IWP and IWC last too short. This could be related to the conversion from cloud ice to snow.

c) the layer-mean IWCs decrease with cloud physical thickness, in opposition to the retrievals and CRM results; This could be caused by the detrainment process. In the SCM detrainment occurs at too thin layer compared to the corresponding CRM simulation. If detrainment occurred in thicker layer, the cloud would be thicker for the same IWP and lower IWC. This would tend to correct the errors.

d) the distribution of layer-mean effective radii covers too narrow a range with a maximum cut-off at about 75 μm indicating the limitation of the SCM's method to determine the effective radius of cloud ice particles.

The assumed uniform distribution of sub-grid scale IWC in the SCM is incorrect. It should be inhomogeneous at a given level. This assumption should contribute to part of the problems found.

REFERENCES

Arakawa, A. and W. H. Schubert, 1974: Interaction of a cumulus ensemble with the large-scale environment, Part I. *J. Atmos. Sci.*, **31**, 674-704.

Beesley, T. A., C. S. Bretherton, C. Jakob, E. L. Andreas, J. M. Intrieri, and T. A. Uttal, 2000: A comparison of the ECMWF forecast model with observations at SHEBA, *J. Geophys. Res.*, accepted 12/99. Available from: ftp://eos.atmos.washington.edu/pub/breth/papers/MBL_clouds/SGEBA1.ps.gz

Chou, M. D., M. J. Suarez, C. H. Ho, M. M. H. Yan, and K. T. Lee, 1998: Parameterization for cloud overlapping and shortwave single scattering properties for use in general circulation and cloud ensemble models. *J. Climate*, **11**, 202-214.

Fu, Q., and K. N. Liou, 1993: Parameterization of the radiative properties of clouds. *J. Atmos. Sci.*, 50, 2008-2025.

Fu, Q., S. K. Krueger, and K. N. Liou, 1995: Interactions of radiation and convection in simulated tropical cloud clusters. *J. Atmos. Sci.*, **52**, 1310-1328.

Grell, G. A., 1993: Prognostic evaluation of assumptions used by cumulus parameterization. *Mon. Wea. Rev.*, **121**, 764-787.

Hsie, E. Y., R. D. Farley, and H. D. Orville, 1980: Numerical simulation of ice phase convective cloud seeding, *J. Appl. Meteor.*, **19**, 950-977.

Kalnay, E., S. J. Lord, and R. D. McPherson, 1998: Maturity of operational numerical weather prediction: medium range. *Bull. Amer. Meteor. Soc.*, **79**, 2753-2769.

Kiehl, J. T., J. J. Hack, G. B. Bonan, B. A. Boville, D. L. Williamson, and P. J. Rasch, 1998: The national center from atmospheric research community climate model CCM3. *J. Climate*, **11**, 1121-1149.

Klein, S., and C. Jakob, 1999: Validation and sensitivities of frontal clouds simulated by the ECMWF model. *Mon. Wea. Rev.*, **127**, 2514-2531.

Krueger, S. K., 1988: Numerical simulation of tropical cumulus clouds and their interaction with the subcloud layer. *J. Atmos. Sci.*, **45**, 2221-2250.

Krueger, S. K., Q. Fu, K. N. Liou, and H-N. S. Chin, 1995c: Improvements of an ice-phase microphysics parameterization for use in numerical simulations of tropical convection. *J. Applied Meteor.,* **34**, 281-287.

Lin, Y. L., R. D. Farley, and H. D. Orville, 1983: Bulk parameterization of the snow field in a cloud model. *J. Climate Appl. Meteor.*, **22**, 1065-1092.

Lord, S. J., H. E. Willoughby and J. M. Piotrowicz, 1984: Role of a parameterized ice-phase microphysics in an axisymmetric tropical cyclone model. *J. Atmos. Sci.*, **41**, 2836-2848.

Luo, Y., S. K. Krueger, G. G. Mace, and K.-M. Xu, 2002: Cirrus Cloud Statistics from a Cloud-Resolving Model Simulation Compared to Cloud Radar Observations. Accepted by *J. Atmos. Sci..*

Mace, G. G., E. E. Clothiaux, and T. P. Ackerman, 2001: The composite characteristics of cirrus clouds; bulk properties revealed by one year of continuous cloud radar data. *J. Climate*, **14**, 2185-2203.

Mace, G. G., T. P. Ackerman, P. Minnis, and D. F. Young, 1998: Cirrus layer microphysical properties derived from surface-based millimeter radar and infrared interferometer data. *J. Geophys. Res.*, 103, 23,207-23,216.

Minnis, P., W. L. Smith, Jr., D. P. Garber, J. K. Ayers, and D. R. Doelling, 1995: Cloud properties derived from GOES-7 for Spring 1994 ARM Intensive Observation Period using Version 1.0.0 of ARM satellite data analysis program. NASA Reference Publication 1366, NASA Langley Research Center, Hampton, VA 23681-0001.

Pan, H.-L., and W.-S. Wu, 1995: Implementing a mass flux convection parameterization package for the NMC medium-range forecast model. National Meteorological Center, Office Note 409, 40 pp. [Available from NCEP/EMC, 5200 Auth Road, Camp Springs MD 20746]

Slingo, A., 1989: A GCM parameterization for the shortwave radiative properties of water clouds. *J. Atmos. Sci.*, **46**, 1419-1427.

Stephens, G. L., 1984: The parameterization of radiation for numerical weather prediction and climate models. *Mon. Wea. Rev.*, **112**, 826-867.

Sundqvist, H., E. Berge, and J. E. Kristjansson, 1989: Condensation and cloud studies with a mesoscale numerical weather prediction model. *Mon. Wea. Rev.*, **117**, 1641-1657.

Taylor, K. E., 2001: Summarizing multiple aspects of model performance in a single diagram. *J. Geophys. Res.,* **106***,* 7183-7192.

Xu, K.-M., and S. K. Krueger, 1991: Evaluation of cloudiness parameterizations using a cumulus ensemble model. *Mon. Wea. Rev.*, **119**, 342-367.

Xu, K.-M., and D. A. Randall, 1995: Impact of interactive radiative transfer on the macroscopic behavior of cumulus ensembles. Part I: Radiation parameterization and sensitivity test. *J. Atmos. Sci.*, **52**, 785-799.

Xu, K.-M., and D. A. Randall, 1996: A semiempirical cloudiness parameterization for use in climate models. *J. Atmos. Sci.*, **53**, 3084-3102.

Xu, K.-M., and D. A. Randall, 2000: Cloud resolving model simulation of the July 1997 IOP: Comparison with ARM data on short, medium, and long subperiods. *Proceedings of the Tenth Atmospheric Radiation Measurement (ARM) Science Team Meeting*, March 13-17, 2000, San Antonio, Texas.

Zhao, Q., and F. H. Carr, 1997: A prognostic cloud scheme for operational NWP models. *Mon. Wea. Rev.*, **125**, 1931-1953.